NUMERICAL SIMULATION OF TUNNEL KILNS APPLIED TO WHITE TILE WITH NATURAL GAS

Renato Oba, renatooba@labcet.ufsc.br
Talita Sauter Possamai, talita@labcet.ufsc.br
Andréa Trombini Nunes, andrea@labcet.ufsc.br
Vicente de Paulo Nicolau, vicente@emc.ufsc.br
Dept. of Mechanical Engineering, Federal University of Santa Catarina 88040-970, Florianópolis, SC, BRAZIL

Abstract. *A model for numerical simulation of a tunnel kiln applied in the ceramic industry is presented. Tunnel kilns are widely employed in brazilian ceramic industry for firing red, construction and some types of white ceramic. Exhibiting simple geometry it can be approximated by a parallelepiped, usually three to five meters high, four to five meters wide and with length varying between 90 to 120 meters. The numerical model solves for a 3D problem with models for energy distribution in the burning zone, the advection of gases inside the furnace and the radiation between ceramic load and refractory walls. Energy losses from the kiln to the surroundings are also solved. As main results the simulation presents the characteristic firing curve of the kiln, temperature distribution in the load, walls and gases, estimated production and distribution of energy flows in the kiln, based in parameters such as fuel and cooling and extraction air flows. These data allow to estimate and optimize energy efficiency and production of the kiln. Experimental data from previous works about tunnel kilns installed in Santa Catarina are used for comparison with the numerical results.*

Keywords*: Numerical simulation, tunnel kilns, energy efficiency, characteristic firing curve, temperature distribution.*

1. TABLE OF SYMBOLS

A	Area $\left[m^2\right]$	Subscripts	
c_p	specific heat at constant pressure $\left[J\ kg^{-1}K^{-1}\right]$	$(-)_{conv}$	convection
h	convection coefficient $\left[W\ m^{-2}K^{-1}\right]$	$(-)_{diff}$	diffusion
k	thermal conductivity $\left[W\ m^{-1}K^{-1}\right]$	$(-)_{ext}$	external
LHV	lower heating value $\left[J\ kg^{-1}\right]$	$(-)_{fr}$	front
$\dot{m}$	mass flux rate $\left[kg\ s^{-1}\right]$	$(-)_{fuel}$	fuel
Q	heat transfer rate $[W]$	$(-)_{gases}$	gases combustion
$q"$	heat flux $\left[W\ m^{-2}\right]$	$(-)_{int}$	inside of the kiln
S	radiation heat transfer rate $[W]$	$(-)_{i}$	index
T	temperature $[K]$	$(-)_{oxi}$	oxidant
V	volume $\left[m^3\right]$	$(-)_{ref}$	reference
Greek letters		$(-)_{sur}$	surface
ε	surface emissivity [-]	$(-)_{rad}$	radiation
σ	Stefan-Boltzmann constant $\left[W\ m^{-2}\ K^{-4}\right]$	$(-)_{w}$	wall

2. INTRODUCTION

Energy costs in the ceramics industry represent a major expenditure. National Association of Ceramic Manufacturers (Anfacer – Brazil) reports that energy costs represent 30% of production costs in the segment (Ferreira et al., 2008).

In the red ceramics industry, the most common kiln found is the tunnel kilns mainly due to the possibility of using different types of fuel for firing a great variety of ceramics products in a continuous production. The most common types of ceramic produced in this kind of kiln are bricks, tiles and construction blocks.

The use of natural gas in the ceramic industry have grown over the last decade fueled by the possibility of a clean burning, free from the presence of soot. Even so the most used fuel is still firewood due to its low cost, representing 50% of energy consumption in this sector in Brazil, followed by natural gas with 20% (National Energy Balance 2010, base year 2009, Brasilia, 2010).

Obtaining numerical accurate information about characteristics of the main variables of an equipment allows the development of sensitivity about the project from the point of view of energy. The large dimension of this type of kiln, it can reach over 200 m length, makes difficult to apply commercial CFD codes due to the high computational demand required. This fact drives the development of specific codes and models to solve the thermal problem involved in the process of burning ceramics.

Caddet *et al*. (1993), Dadam *et al*. (2003), and Jahn *et al*. (2005) present the energy distribution in tunnel kilns used in the Brazilian industry, based in experimental studies.

This work presents a numerical model developed in FORTRAN to estimate the energy distribution inside the furnace and the heat transfers involved in the process of firing red ceramic in a tunnel kiln. The code is based in the method of finite volume. The concept of plane plates is used to calculate the radiation heat transfer. For solving the species composition and temperature, a combustion model coupled with the program STANJAN (Stanford University) is used.

3. KILN SET UP

The kiln schematic geometry is presented in Figures 1 and 2. It is idealized as a rectangular structure with constant width and height of 3 m and 90 length. Its walls are composed by three layers; two of brick and the one of refractory bricks, totalizing 0.4 m width. The internal cavity where the ceramic load passes through is 1.9 m height and 2.2 m width. The load itself is idealized as a solid but porous parallelepiped with dimensions of 1.6 and 1.8 m of height and width respectively. It is mounted on a solid furniture that isolates the load from the bottom of the kiln. The lorry is 0.4 m height and 1.8 m width. Figure 2 presents the load's drawings. The fuel used is natural gas.

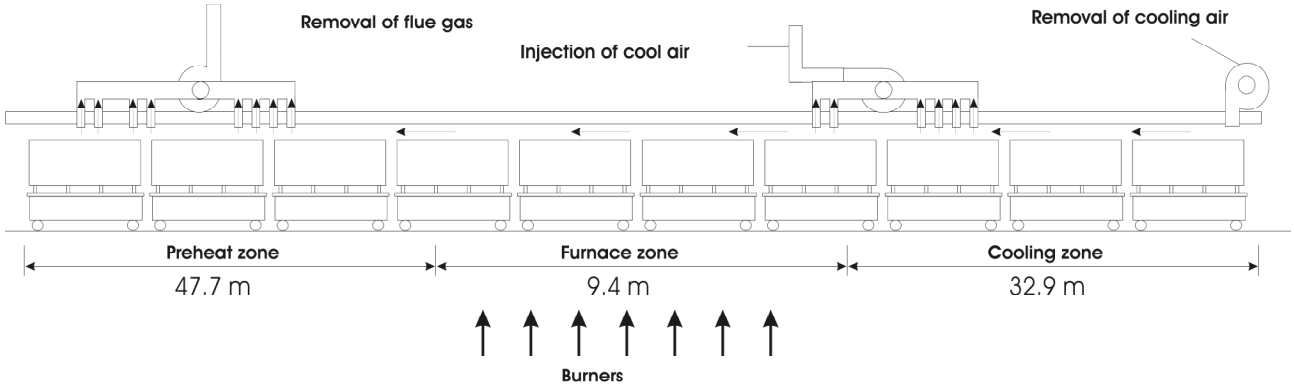

Figure 1. Kiln geometry

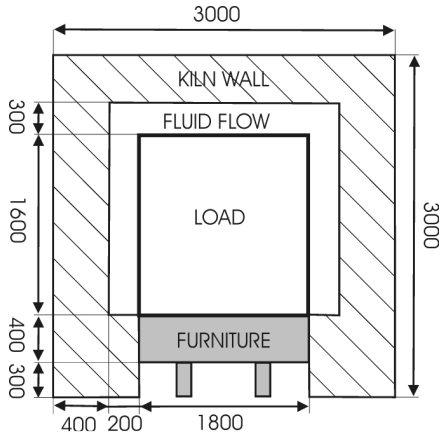

Figure 2. Dimensions of the furnace, load and lorry

Three main zones compose the kiln: preheat, furnace and cooling zone. In the first region the load is heated by the hot gases coming from the furnace zone, preparing it to be fired in the next zone, as well as removing humidity from the

load. This heating must be slow and controlled to avoid cracking, bubbles, or tile´s break. In the furnace zone, the load is sintered, all its characteristics - as strength and color – depend on the temperature and time spending in this zone. Ten burners (five in each side) are responsible for the natural gas combustion. The last zone, the cooling zone, is responsible for the decreasing of the load's temperature. The cooling usually occurs into three steps; the first step is a quick drop in temperature by air injection directly into the tile, in the second step air passes through the furnace with no contact to the load, cooling it even more, but in a slow manner, the hot air remaining with the load is sucked out of the kiln in the third step making possible for the load to be removed from the furnace. Figure 3 shows the directions of movement of the ceramic load and the flow of hot and cool gas idealized in this study inside the tunnel kiln.

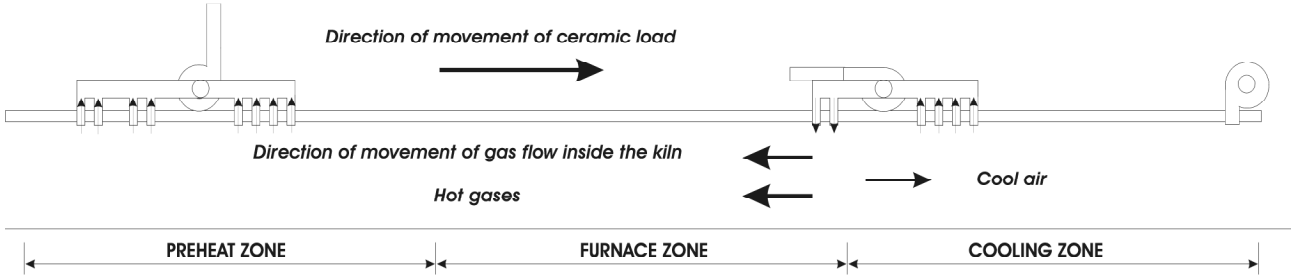

Figure 3. Ceramic load and flow directions inside the tunnel kiln.

4. MODEL DESCRIPTION

The domain of resolution is formed by the furniture, the tile load, the walls, composed by the three layers, and the cavity between the wall and the load - filled with fluid flow. The numerical model is based on the method of finite volume. Figure 4 shows the domain of resolution divided in sub-domains. Each sub-domain is divided in several volumes where the equations that describe the physical phenomena are solved. The left image is a transversal cut while the right one is a longitudinal.

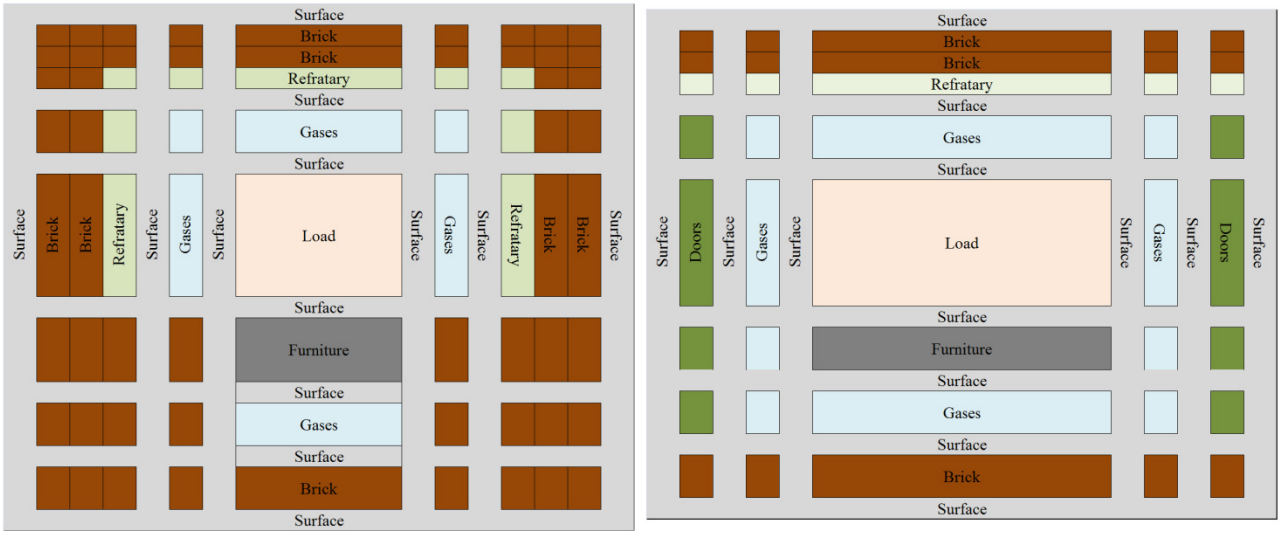

Figure 4. Intern sub-domains.

4.1. HEAT TRANSFER MODELS

The heat transfer from the kiln walls to its surroundings by radiation and convection are modeled by equations 1 and 2, respectively.

$$Q_{conv} = h_{ext} A_{sur} (T_{sur} - T_{ext}) \tag{1}$$

$$Q_{rad} = \varepsilon \sigma A (T_{sur}^4 - T_{ext}^4) \tag{2}$$

The Navier Stokes equations are not solved for the fluid flow inside the kiln, being the velocity and the direction of the same prescribed, based on empirical data. The sense of motion of the flow prescribed is the one presented in figure 3. The thermal energy equation, equation 3, is solved for the fluid flow, enclosing energy exchanges with the ceramic load and the walls through convection and with itself by mass advection. For a volume with no fluid-solid interface, the convection energy flux q''_{conv} is considered equal to zero. No energy diffusion inside the flow is considered. For a volume with a solid-fluid interface, i.e. adjacent to the ceramic load, the kiln wall or the furniture, the convection energy flux assumes the form of equation 4.

$$\frac{\partial}{\partial x_i}\left(\rho U_i T\right) = -\frac{\partial}{\partial x_i}\left(q''_{conv,i}\right) \tag{3}$$

$$q''_{conv,i} = h_{int}\left(T_{w,i} - T\right) \tag{4}$$

For the walls and furniture, the thermal energy equation reduces to equation 5, where when applied to a volume with an interface fluid-solid, the energy flux q''_{conv} in the interface reduces to equation 4 and the radiation energy source is defined as equation 6. For a volume with no fluid-solid interface, the convection energy flux q''_{conv} is considered equal to zero. The energy flux due to heat diffusion q''_{diff} is defined by equation 7. The radiation model applied to the inside of the kiln only considers exchange by radiation between the kiln wall and the ceramic load through the concept of plane plate (Incropera and DeWitt, 2002), where a surface only sees the surface positioned directly in front of it. For volumes with no solid-fluid interface, i.e. inside the kiln walls and inside the load, the radiation source reduces to zero. The fluid flow is considered as a non participating media in the radiation exchanges.

$$\frac{\partial}{\partial x_i}\left(q''_{conv,i}\right) + \frac{\partial}{\partial x_i}\left(q''_{diff,i}\right) + \frac{S_{rad}}{V} = 0 \tag{5}$$

$$S_{rad} = \sigma\varepsilon A\left(T^4 - T_{fr}^4\right) \tag{6}$$

$$q''_{diff,i} = -k\frac{\partial T}{\partial x_i} \tag{7}$$

The ceramic load is considered as a porous solid. To solve the temperature field, the thermal energy equation reduces to equation 8, with the same considerations to the heat flux and radiation energy source as for the wall and furniture. However, for the load, the convection energy flux does not reduce to zero in the solid-solid interfaces, being present in all volumes inside the load due to the porosity of the solid.

$$\frac{\partial}{\partial x_i}\left(\rho U_i T\right) = -\frac{\partial}{\partial x_i}\left(q''_{conv,i}\right) - \frac{\partial}{\partial x_i}\left(q''_{diff,i}\right) - \frac{S_{rad}}{V} \tag{8}$$

Figure 5 shows the heat transfer modes considered in each sub-domain. The properties used in this study are listed in Table 1.

Table 1 - Properties

Properties	Value	Unit
Internal convection heat transfer coefficient, h_{int}	100	$W.m^{-2}.K^{-1}$
External convection heat transfer coefficient, h_{ext}	10	$W.m^{-2}.K^{-1}$
Kiln walls and ceramic load emissivity, ε	0.8	-
Stefan-Boltzmann constant, σ	$5.67x10^{-8}$	$Wm^{-2}.K^{-4}$
Thermal conductivity of the walls, k	0.25	$W.m^{-1}.K^{-1}$
Thermal conductivity of the furniture, k	0.2	$Wm^{-1}.K^{-1}$
Thermal conductivity of the ceramic load, k	0.15	$W.m^{-1}.K^{-1}$
Specific heat of the ceramic load, c_p	875	$J.kg.K^{-1}$
Specific heat of the furniture, c_p	875	$J.kg.K^{-1}$
Lower heating value of natural gas, LHV	49.22	$M.J.kg^{-1}$

Reference temperature, T_{ref}	27	ºC
Specific heat at constant pressure of the flue gas, c_p	1500	$J.kg^{-1}.K^{-1}$

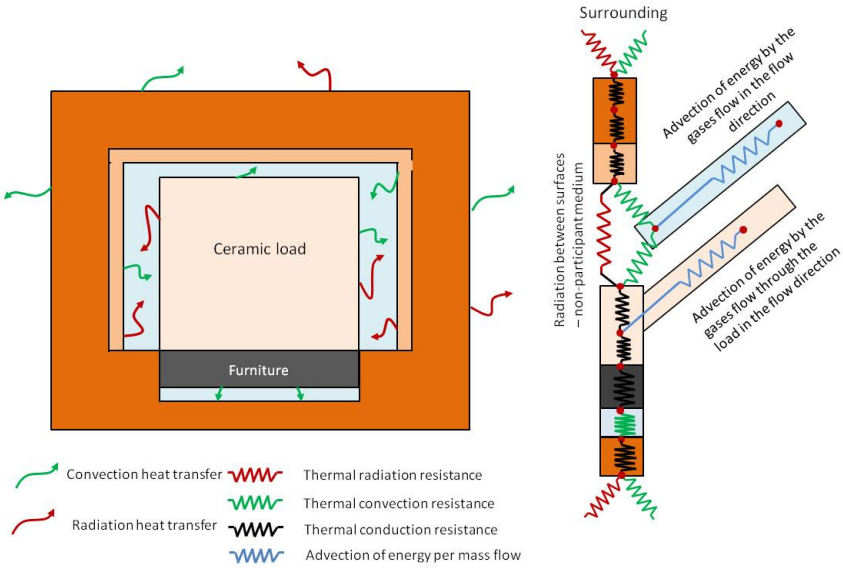

Figure 5. Heat transfers and thermal resistances in a transverse section of the furnace.

4.2. COMBUSTION MODEL AND FLOW INJECTION

The burners are modeled as uniform injections of hot gases through the lateral walls of the kiln in the furnace zone (Figure 6). The inlet temperature of the gases is solved through equation 9.

Equations 10 and 11 are also applied to this routine to define the mass flow inside the kiln and the air/fuel relation.

$$\dot{m}_{fuel} \cdot LHV = \dot{m}_{gases}\ c_{p,gases}(T_{gases} - T_{ref}) \tag{9}$$

$$\dot{m}_{gases} = \dot{m}_{fuel} + \dot{m}_{oxi} \tag{10}$$

$$\Phi = \frac{\dot{m}_{oxi}}{\dot{m}_{fuel}} \tag{11}$$

The specific heat of the gases $c_{p_{gases}}$ is calculated by the STANJAN program - Chemical Equilibrium Solver, Stanford University, version 3.95. For the problem in study, the stoichiometric coefficient ϕ is assumed to be 17,17 for combustion with natural gas and air.

In the cooling zone, cool air is injected at the surroundings temperature. To model the chimneys in the preheat and cooling zones, there are two extractions of gases, one in the first row of volumes of the mesh and the other in the last row. The air injection in any region of the kiln is modeled as uniform through the walls along the entire region. The total mass flow injected is divided by the numbers of lateral volumes that the region has, as can be seen in Figure 6.

The mesh used for this study is composed of 1,250,000 volumes, not uniform. The number of volumes in each direction is 50 in width, 50 in height and 500 in length. The UDS scheme is adopted to solve the advection problem. For the energy diffusion terms, an approximation by finite differences is applied and the Gauss Seidel method is used as the mathematical solver, with the implicit method.

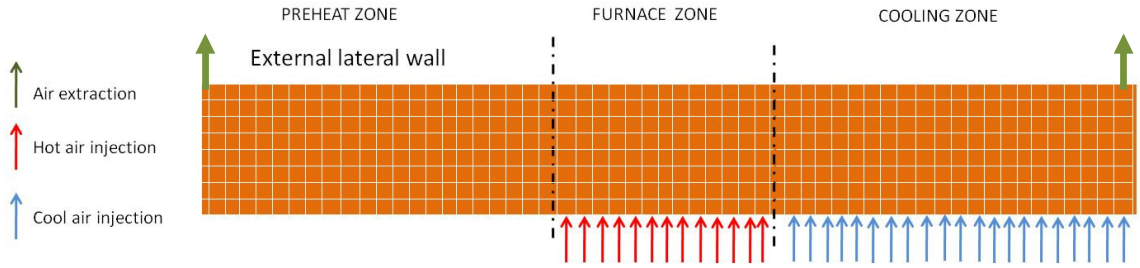

Figure 6. Air/gases injection.

4.3. THE AIR AND GASES FLOW MODEL

A factor called *f* is used to determine the flow of gases in the transverse direction entering the load as shown in Figure 7. This factor varies from 0 to 1, making it possible to simulate different cases as high pressure suction by the fans (high *f* factor), or tiles far from each other (low *f* factor), and how these cases interfere in the curve temperature of the gases inside the kiln. A factor of 0.2 was adopted for the cases solved for this study.

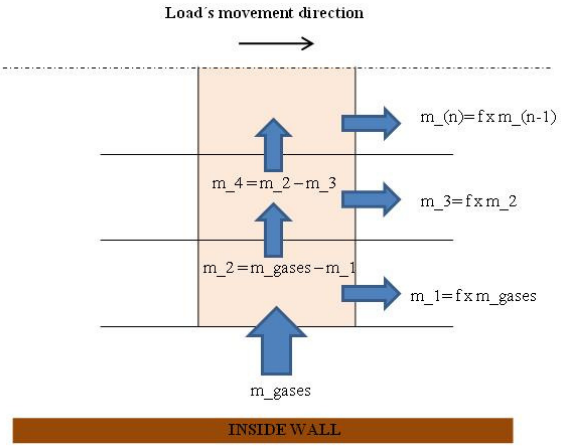

Figure 7. *f* factor.

5. RESULTS

The numerical results estimates temperature fields inside and outside of the kiln, as well as the energy distribution inside the kiln allowing the user to evaluate the kiln´s efficiency and identify possible hot spots in the kiln or in the load.

For comparison, two different fuel mass flows were tested. The two cases are: 0.0304 and 0.0604 kg/s of natural gas. The stoichiometric air flow necessary for the combustion are 0.9558 and 1.8989 kg/s respectively.

Figure 8 presents the temperature curve for the gases inside the kiln for the two cases. As expected, the greater the fuel consumption the greater the temperature. The points where the curve changes its direction indicate the beginning and ending of the furnace zone, while the quick drop in temperature indicates air injection in the cooling zone.

Figure 9 and 10 shows the temperature field in three transverse sections of the kiln, one in each zone for the two cases of fuel consumption. All transverse sections plotted correspond to the middle of each zone, the load is supposed continuous from 0,6 m to 2,4 m of the kiln´s width and 0,7 m to 2,3 m of its height, while the furniture has the same width and 0,7 m height.

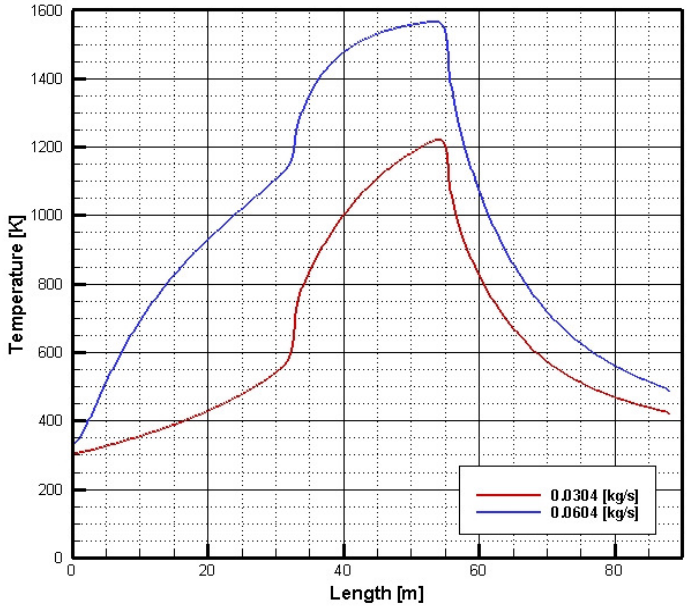

Figure 8. Temperature curve of flow inside the kiln.

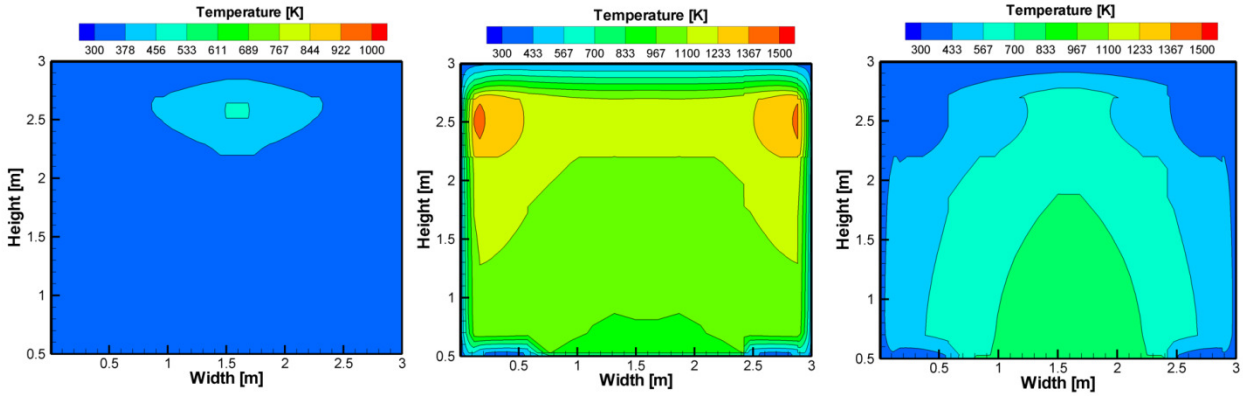

Figure 9. Heating (left), combustion (middle) and cooling (right) transverse section of the kiln – 0.0304kg/s of natural gas.

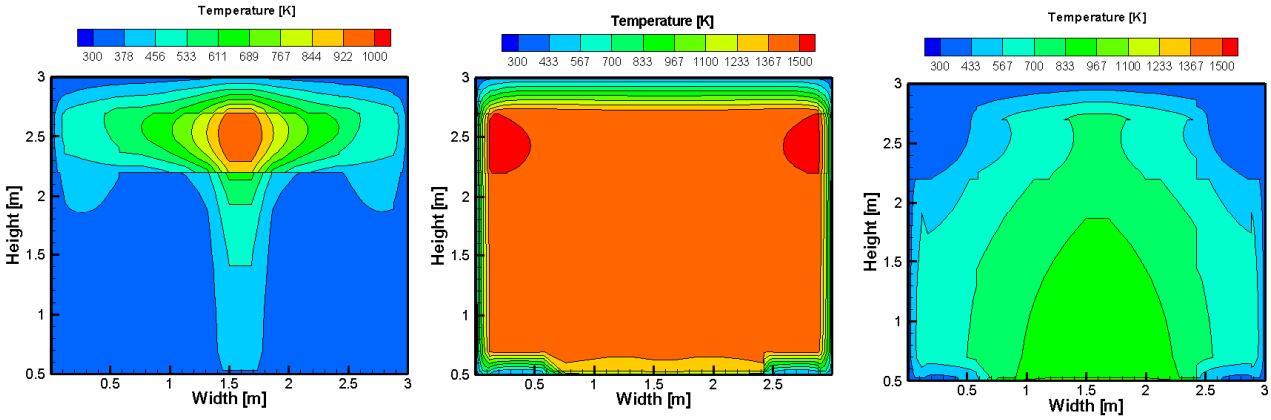

Figure 10. Heating (left), combustion (middle) and cooling (right) transverse section of the kiln – 0.0604kg/s of natural gas.

In the combustion zone the highest temperatures are found in the upper edges near to the combustion gases, according to the model adopted. The load´s temperature distribution for the same cases is shown in Figures 11 and 12.

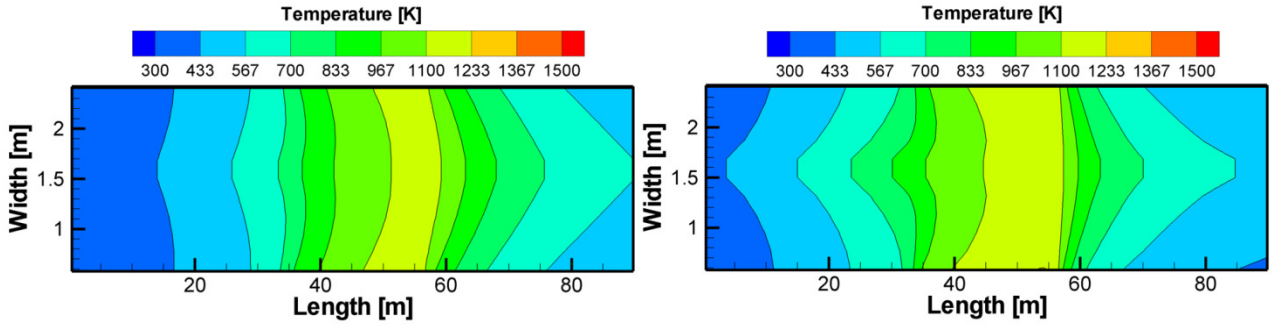

Figure 11. Load´s middle (left) and surface (right) temperature distribution for 0.0304 kg/s of natural gas.

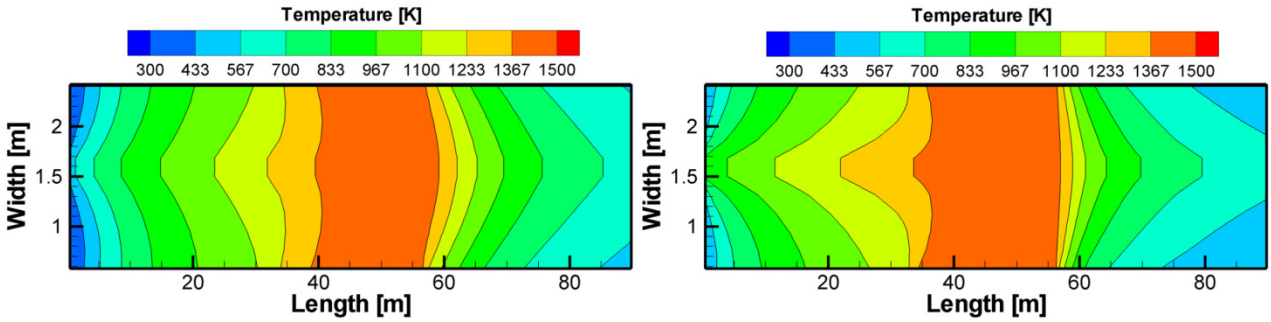

Figure 12. Load´s middle (left) and surface (right) temperature distribution for 0.0604 kg/s of natural gas.

The fuel comsuption affects diretly the temperature of the load, more visible in the furnace zone. Figures 13 shows the external temperature for the two cases. The top image is from the lateral wall and the bottom is from the roof.

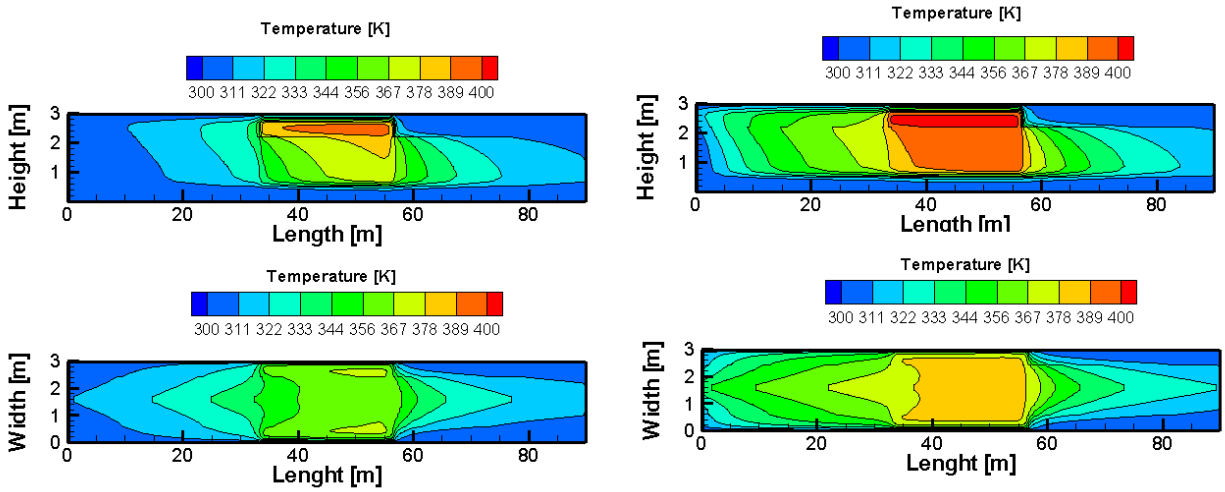

Figure 13. Outside temperature of the walls (side and roof) for 0.0304 (left) and 0.0604 (right) kg/s.

The temperatures on the side of the kiln do not vary greatly from the ceiling´s, with the highest temperatures occurring in the furnace zone. The insulation effect of the furnace can be seen in the bottom region of the external temperature of side wall. The difference between the fuel consumption is noticed on the higher temperatures with the case of more fuel, as expected.

Another important tool to analyze the kiln is by its energy distribution. The global energy balance of the kiln is presented in Table 4, for the two cases tested. Experimental data from the works of Caddet *et al*. (1993), Dadam *et al*. (2003), and Jahn *et al*. (2005) are displayed for comparison with the numerical results.

Table 4. Energy balance for the cases studied.

	Natural gas mass flow [kg/s]				Dadam, 2003	Jahn, 2005	Caddet, 1993
	0.0304		0.0604				
Incoming energy							
Description	[kW]	[%]	[kW]	[%]	[%]	[%]	[%]
Combustion energy	1241.6	100.0	2466.9	100.0	-	-	-
Out coming energy							
Gases – heating region chimney	48.3	3.89	648.6	26.29	34.3	11.7	39.9
Cooling air	572.7	46.13	805.6	32.66	34.7	53.2	33.7
Tile load	236.2	19.03	330.6	13.40	4.5	5.0	0.2
Furniture	34.2	2.76	53.9	2.18	-	-	-
Wall	350.2	28.21	629.28	25.51	7.6	4.8	13.2
Others	-	-	-	-	16.5	25.3	12.8
Energy balance [kW]							
Incoming	1241.6		2466.9		-	-	-
Out coming	1241.7		2467.9		-	-	-
Error [%]	0.02		-0.04		-	-	-

Following each energy quantity there is its corresponding fraction related to the amount of energy released by the natural gas combustion. While the energy lost by the preheat chimney increases roughly by the increase of the fuel´s consumption, all the others out coming's fractions present a more subtle variation, with the tendency to decrease their value by the increasing in the fuel mass flow. As can be seen by the temperature distribution of the load and the gases inside the furnace, the greater the consumption of the fuel, the greater the temperature in the beginning of the kiln, causing the chimney to expel hotter gases, thereby losing more energy by it. Comparing with energy distribution from the works of Caddet *et al*. (1993), Dadam *et al*. (2003), and Jahn *et al*. (2005), some discrepancies are observed mostly in the energy loss through the walls and the tile load. The case with 0.0604 kg/s of fuel is more consistent with the experimental data, probably being a value of mass flow of fuel nearer of the one from the operating kilns.

6. CONCLUSION

The results above present the possible features that can be obtained by the numerical model developed. Although the numerical prediction given is consistent, experimental data of the kiln in operation condition is necessary for real validation. Once tunnel kilns are widely used in industry, a model capable of estimating the temperature and energy distribution and kiln's efficiency is a helpful tool for predictions as well as energy optimizations.

7. REFERENCES

Caddet. "Insulated Carts for Tunnel Kilns in Brick Manufacture". Center for the Analysis and Dissemination of Demonstrated Energy Technologies, March, 1993.

Dadam, A.P., Nicolau, V.P., Hartke R.F., Kawaguti, W. M., Jahn,T.G, Lehmkuhl, W. A., Santos, G.M. "Análise Numérica e Experimental de um Forno Túnel Utilizado em Cerâmica Vermelha", Congresso Brasileiro de Engenharia e Ciências Térmicas, Caxambu – MG, 2002, artigo CIT02-0533, 10p.

Ferreira S. I. C., Alexandre N. M. D., Vitorino A. A. L. F., "Otimização Energética de um Forno na Indústria Cerâmica", Cerâmica Industrial. 13 (1/2) January/April, 2008

Jahn, T.G., "Acquirement of experimental data and thermal simulation in rollers kiln with natural gas", Msc thesis, Florianopolis, SC, 2007, Federal University of Santa Catarina (In Portuguese).

Incropera, F. P., Dewitt, D. P. Fundamentals of heat and mass transfer. 5. ed. John Wiley & Sons, Inc, 2002.

8. RESPONSIBILITY NOTICE

The authors are the only responsible for the printed material included in this paper.